

# The electromagnetic pulse effect injection experiment and simulation modeling analysis of band-pass filter

C Fei <sup>a</sup>, X D Wei <sup>b</sup>

Electromagnetic Pulse Laboratory, Xi'an Research Institute of high-tech, Xi'an 710025, China;  
<sup>a</sup> caofei101@126.com, <sup>b</sup> 583196838@qq.com

## Abstract

As an important component of the radio frequency front end of various wireless communication equipment, band-pass filters are often the first to bear the brunt in the environment of high-power electromagnetic pulses. The instantaneous large current generated by the electromagnetic pulse coupled by the antenna will easily cause interference or even damage to the subsequent sensitive devices once it breaks down the filter and leaks. Select a typical mid-band pass filter, carry out component-level double exponential pulse current injection experiments, and analyze its input and output current characteristics; On this basis, the double exponential pulse source and band-pass filter are simulated and modeled, and the injection test model is built on the simulation software. The simulation injection test results are compared and analyzed with the actual situation, which verifies the accuracy of the model well.

## Keywords

Band pass filter, injection test, electromagnetic pulse.

## 1. Introduction

Modern electronic devices are susceptible to high-power electromagnetic environments. Especially in the radio frequency front-end circuit of the receiver, a filter is often placed in the front end of each amplifier for protection, so it is very important to study the electromagnetic pulse effect of the filter. In this paper, a certain type of band-pass filter is used as the effect test object, using the pulse current injection method to inject a double exponential pulse with adjustable voltage, the rising edge of the waveform parameter is 20ns, and the pulse width is 500ns. Based on the analysis of the results of the filter injection test, simulation modeling of the double exponential pulse source, band-pass filter and other modules is carried out, and the entire band-pass filter injection test is implemented on the simulation software.

## 2. Pulse Current Injection Test of Band-Pass Filter

The mid-band pass filter is generally composed of lumped components such as capacitors and inductors. The double-exponential pulse injection test scheme is shown in Figure 1. In the scheme, the 20/500ns double exponential pulse source is connected to the mid-band pass filter, and the end is connected to a 50 ohm matched load. In the experiment, the output voltage of the pulse source was adjusted, the input and output currents of the effectors were collected by an oscilloscope, and the waveforms under each pulse injection were recorded.

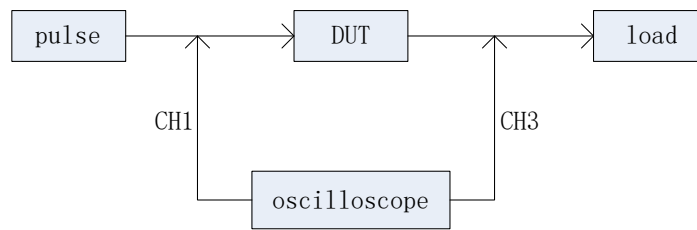
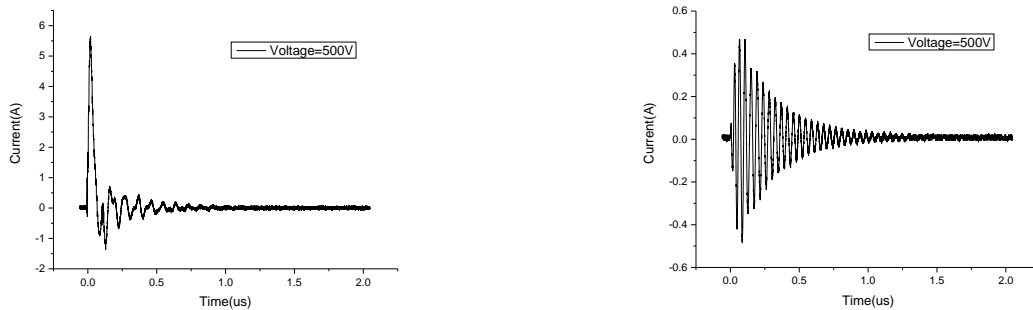


Figure 1: Current injection experimental diagram

Figure 2 shows the typical waveforms of input and output currents when the output voltage of the pulse source is 500V. When the injection voltage is equal to 500V, the peak input current is 5.6A. After the effector is added, the entire circuit network does not match. The input current waveform is a double exponential oscillating waveform, and the output current peak value is 0.5A, which is an order of magnitude lower than the input current, greatly reducing the threat to the downstream devices, and showing obvious filtering characteristics.



(a) Input current waveform

(b) Output current waveform

Figure 2: Typical waveform of band-pass filter pulse injection test

### 3. Simulation Realization of Double Exponential Pulse Current Injection Test for Band Pass Filter

#### 3.1. Double exponential pulse source circuit modeling

By testing the output current of the pulse source short circuit and connecting 50 ohm load, it is found that when the output voltage is 500V, the peak value of the output current in the short circuit state is 10A, and it is a standard 20/500ns waveform. When the load end is connected to a 50 ohm load, the peak output current is 5A, the current waveform will expand, and the pulse width will increase. It is judged that the internal resistance of the pulse source is 50 ohms. According to the tested parameters, the pulse source circuit model based on ADS circuit simulation software is shown in Figure 3. In addition to adding internal resistance to the circuit, two steepening capacitors are also connected in parallel to improve the input current waveform. And in general, the resistance also needs an inductance in series to simulate the circuit parasitic parameters that exist in the real circuit. The output current waveform of the pulse source obtained by the simulation is compared with the actual test waveform under the same level as shown in Figure 4. It can be seen from the figure that there is a high degree of coincidence between the two, and the waveform is basically completely fitted, which verifies the accuracy of the model.

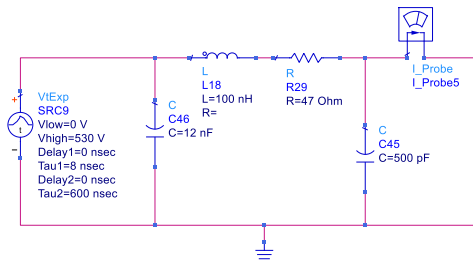


Figure 3: Pulse source circuit model

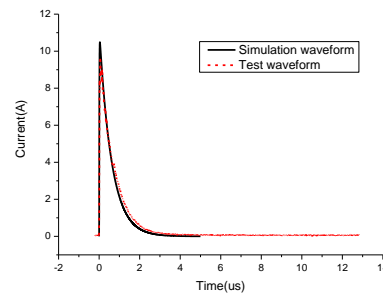


Figure 4: Pulse source simulation and test current

### 3.2. Bandpass filter circuit modeling

When designing a filter, it is usually regarded as a two-port network. An ideal filter will completely block out-of-band signals and completely pass in-band signals. According to the working frequency band of the filter, it can be divided into: low-pass filter, high-pass filter, band-stop filter, and band-pass filter. However, there is no ideal filter in the actual design. It can only produce a large attenuation of the unwanted frequency signal, and pass the required signal in the frequency band with a small attenuation. And use some indicators of the filter to describe the relevant response characteristics. The signal processed by the mid-band-pass filter is an intermediate-frequency signal, and the center frequency is selected as 70MHz. The circuit modeling is shown in Figure 5 according to a mid-band-pass filter used in the experiment. The S21 parameter curve obtained by testing the mid-band pass filter with a vector network analyzer is shown in Figure 6. The measured 3dB passband bandwidth of the filter is 20MHz~90MHz, and there is almost no attenuation in the passband.



Figure 5: Bandpass filter physical picture

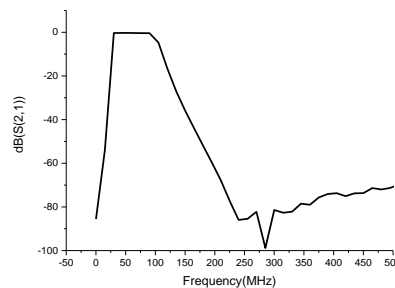


Figure 6: Bandpass filter S21 test curve

Since the working frequency of the mid-band pass filter is low, the distribution parameters of the circuit have less influence, and lumped elements such as capacitors and resistors are commonly used to form the filter. Among them, the low-pass prototype filter composed of lumped elements is the basis for modern network synthesis methods to design filters, and the transmission characteristics of other types of filters can be derived from the low-pass prototype. In the simulation modeling process of the mid-band-pass filter in this article, two low-pass prototype filters are first established, and then one of the pass frequency changes is converted into a high-pass filter, and finally the two filters are connected in series to obtain a band-pass filter. The core of the above modeling process is to design two low-pass prototype filters. The steps can be briefly divided into three steps:

step one:

The band-pass filter can be seen as a series connection of a low-pass and a high-pass filter. The upper and lower side frequencies of the band-pass filter are used as the cut-off frequencies of the two low-pass filters. The cut-off frequency is 90MHz, and the maximum ripple in the filter band is 0.01dB. The cut-off frequency is 20MHz, the maximum ripple in the filter band is 0.1dB,

and finally the low-pass filter is converted into a high-pass filter through frequency conversion. Considering that when the frequency is reduced to 10MHz or increased to 200MHz, the response of the band-pass filter is attenuated to -60dB, and the number of reactive components n=7 is selected.

Step two:

In the process of low-pass prototype filter design, the normalized frequency is usually used instead of the real frequency, and the normalized signal source internal resistance or load replaces the real impedance (usually 50ohms), which is  $\omega'_1=1, g_0=1$ . Normalize the value of each component in the low-pass prototype to  $g_0$ , and the conversion formula of its real resistance, inductance and capacitance is:

$$R = \left(\frac{R_0}{R'_0}\right) \cdot R' \tag{1}$$

$$L = \left(\frac{R_0}{R'_0}\right) \left(\frac{\omega'_1}{\omega_1}\right) \cdot L' \tag{2}$$

$$C = \left(\frac{R'_0}{R_0}\right) \left(\frac{\omega'_1}{\omega_1}\right) \cdot C' \tag{3}$$

In the above formula, the amount with "skimming" is the normalized amount that can be obtained by looking up the table, and the amount without "skimming" is the actual component value. Generally speaking, in the above formula,  $\omega'_1=1, g_0=R'_0=1$ . Now the normalized value of each component when the number of components is n=7 and the maximum ripple is 0.01 and 0.1 respectively by looking up the table is shown in the table below.

Table 1: Normalized value of low-pass prototype lumped parameter when n=7

Maximum ripple	$g_1$	$g_2$	$g_3$	$g_4$	$g_5$	$g_6$	$g_7$
0.01dB	0.7969	1.3924	1.7481	1.6331	1.7481	1.3924	0.7969
0.1dB	1.1811	1.4228	2.0966	1.5733	2.0966	1.4228	1.1811

Step three:

The low-pass prototype filter corresponding to the cut-off frequency of 90MHz uses a capacitor input circuit as shown in Figure 7. Table 2 shows the actual value of each component obtained by substituting relevant parameters into the formula.

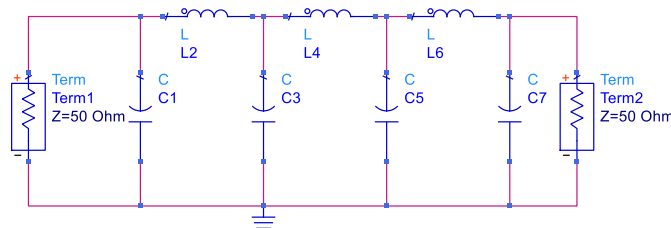


Figure 7: Capacitor input ladder network structure

Table 2: The true value of capacitive input component

$C_1$	$L_2$	$C_3$	$L_4$	$C_5$	$L_6$	$C_7$
28.2pF	123.1nH	61.8pF	144.4nH	61.8pF	123.1nH	28.2pF

The low-pass prototype filter corresponding to the cut-off frequency of 20MHz uses a capacitor input circuit as shown in Figure 8. Table 3 shows the actual value of each component obtained by substituting relevant parameters into the formula.

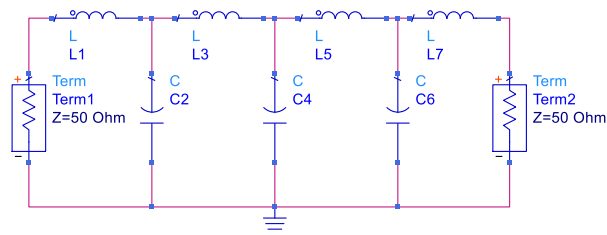


Figure 8: Inductance input type ladder network structure

Table 3: The true value of inductance input component

$L_1$	$C_2$	$L_3$	$C_4$	$L_5$	$C_6$	$L_7$
469.9nH	226.4pF	834.2nH	250.4pF	834.2nH	226.4pF	469.9nH

In the next step, the low-pass filter corresponding to the cutoff frequency of 20MHz is converted to a high-pass filter. The angular frequency variable of the low-pass prototype filter is  $\omega'$ , the cut-off frequency is  $\omega'_1$ , the angular frequency variable of the high-pass filter is  $\omega$ , the cut-off frequency is  $\omega_1$ , and the transformation between the two is

$$\omega' = -\frac{\omega'_1 \cdot \omega_1}{\omega} \tag{4}$$

Correspondingly, the inductance in the low-pass prototype filter is transformed into the capacitance in the high-pass filter, and the capacitance is transformed into inductance. The transformation formula is

$$C = \frac{1}{\omega'_1 \cdot \omega_1 \cdot L'} \tag{5}$$

$$L = \frac{1}{\omega'_1 \cdot \omega_1 \cdot C'} \tag{6}$$

Substituting the component values in Table 3 into the formula, the cut-off frequency of the converted high-pass filter remains unchanged, that is,  $\omega_1 = \omega'_1 = 2\pi f_1$ . The converted high-pass filter is connected in series with another low-pass filter, and the cut-off frequencies of the two filters correspond to the upper and lower side frequencies of the mid-band pass filter, respectively. After proper fine-tuning of the circuit component parameters, the final filter circuit model is shown in Figure 9.

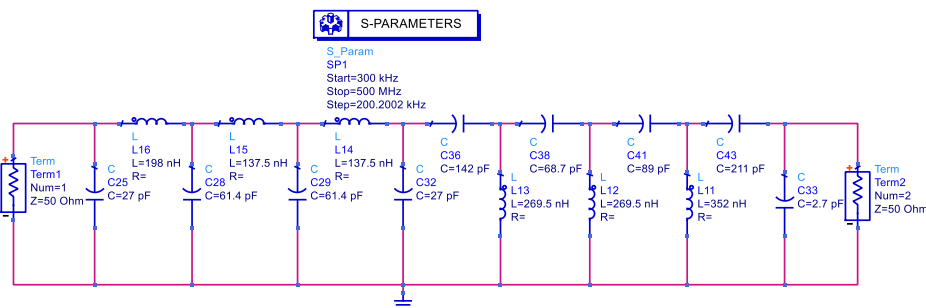


Figure 9: Bandpass filter circuit diagram

Comparing the S21 parameters obtained by circuit simulation with the real object is shown in Figure 10. It can be seen from the figure that the 3dB passband bandwidth of the simulation curve is slightly larger than the actual measurement, but the two curves fit well in general and meet the circuit design requirements.

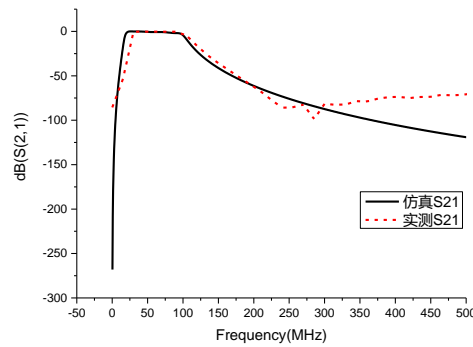
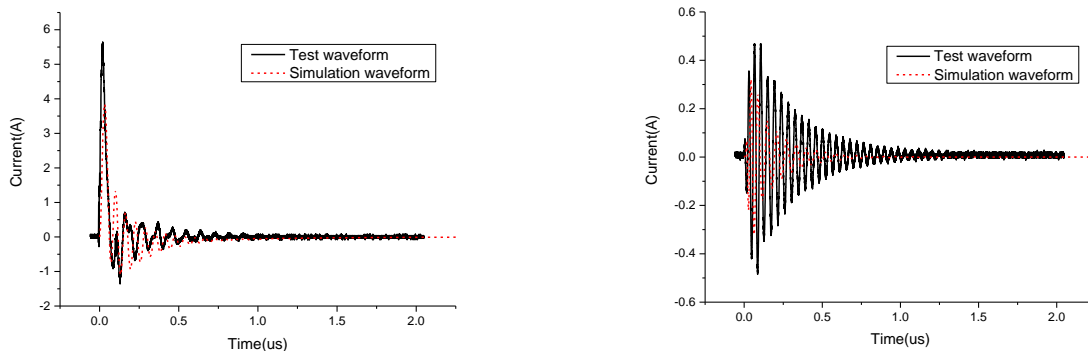


Figure 10: Comparison of simulation modeling curves of bandpass filter

### 3.3. Pulse source injection experiment simulation of band-pass filter

By connecting the pulse source model with the band-pass filter model, the simulation results of the pulse injection experiment are obtained. The comparison between the input and output current waveform and the actual test curve is shown in Figure 11. It can be seen from the figure that there is still a gap between the results obtained by the simulation test and the actual situation. Although the waveform characteristics and change trends are consistent, they are slightly smaller than the actual test curve as a whole, and can be adjusted by adjusting the output voltage of the pulse source simulation model.



(a) Input current waveform

(b) Output current waveform

Figure 11: Typical waveforms for simulation and testing of band-pass filter injection test

## 4. Conclusion

In this paper, the double exponential pulse injection source is selected, and the injection experiment is carried out with a typical band-pass filter as the object. The whole experiment was realized by circuit simulation software, and the circuit modeling process of pulse source and band-pass filter was introduced. The input and output current waveforms obtained by the device simulation are compared and fitted with the actual ones, which verifies the accuracy of the model establishment. By building a simulation model of the band-pass filter pulse injection experiment, it can provide a certain reference and reference significance for the electromagnetic pulse effect experiment of such devices.

## References

[1] Baowei Nie: The Correlation between Different Intensity Electromagnetic Pulse Parameters and Integrated Circuit Damage (M.D., Xidian University, China 2019), p.28.

- [2] Z Shouyang, J Yu, and L Yanping: Study on the Coupling Effect of High Altitude Nuclear Electromagnetic Pulse on Transformer, Electric Porcelain Surge Arrester, Vol. 5 (2019) No.3, p.15-20.
- [3] X Yanzhao, W Z Ji, and W Q Shu: High-altitude nuclear explosion electromagnetic pulse waveform standard and characteristic analysis, Power Laser and Particle Beam, Vol. 15 (2008) No.8, p.781-787.
- [4] L Xinke: Electromagnetic Pulse Coupling and Protection (M.D., Xidian University, China 2009), p.48.
- [5] W T Shun: Nuclear electromagnetic pulse interference and protection technology, Flight design, Vol. 4 (2000) No.4, p.33-39.
- [6] L Xia: Research on Strong Electromagnetic Pulse Shielding and Protection of Electronic Equipment (M.D., Harbin Institute of Technology, China 2017), p.44.
- [7] H Pengwei: Research on Key Technologies of RF Front End Anti-Strong Electromagnetic Pulse (M.D., Xidian University, China 2018), p.35.
- [8] Z Tiancheng, D Dazhi, and F Zhenhong: Analysis of the Mechanism of Nuclear Explosion Electromagnetic Pulse on RF Front End, Journal of Microwaves, Vol. 34 (2018) No.S2, p.443-445.
- [9] J Jianming: Computational Electromagnetism, Second Edition (Publishing House of Electronics Industry, China 2018).
- [10] Zhiliang T, Yanan L, and Peijiao S: Research Progress on Strong Electromagnetic Pulse Protection of RF Front End, Journal of Beijing Institute of Technology, Vol. 40 (2020) No.3, p.231-242.